Materials International
Open-Access Journal (ISSN: 2668-5728)

Article
Volume 7, Issue 3, 2025, 23
https://doi.org/10.33263/Materials73.023

Development and Optimization of Semi-Interpenetrating Polymer Network Microspheres for Sustained Release of Metformin Hydrochloride

Archana G [1], Sasikala M [1], Adilakshmi P [1], Sravya Sri R [1], Swathi T [1], Shaikshavali S [1], Jyosna Doniparthi [1,*]

[1] S.K.U. College of Pharmaceutical Sciences, S.K. University, Anantapur-515003, India
* Correspondence: jyosna.gms@gmail.com;

Received: 28.10.2024; Accepted: 20.08.2025; Published: 10.09.2025

Abstract: This study aimed to design novel semi-interpenetrating microspheres to achieve extended Metformin HCl (MTH) release and improve drug adherence for type II diabetes treatment. Metformin's high water solubility poses challenges for sustained delivery. Gelatin (GE) and hydroxyethyl cellulose (HEC) semi-interpenetrating microspheres were developed using a central composite design. Optimizing the effects of GE, HEC, and glutaraldehyde (GA) concentrations on entrapment efficiency, particle size, and 12-hour drug release was achieved using Design-Expert software. The optimal formulation (F21) — consisting of 4.24% v/v GA, 26.98% w/v GE, and 79.85% w/v HEC — exhibited an entrapment efficiency of 68.4%, a cumulative drug release of 70.7% at 12 hours, and a particle size of 126.8 μm. The release kinetics followed first-order non-Fickian diffusion. SEM analysis confirmed round microspheres with rough, fissured surfaces. FTIR and DSC studies confirmed drug-polymer compatibility. These findings demonstrate that GE–HEC semi-IPN microspheres can significantly extend MTH release, potentially enhancing patient adherence. Further in vivo investigations are warranted to confirm clinical relevance.

Keywords: semi-IPN; microspheres; prolonged release; design expert.

1. Introduction

Over the past three decades, diabetes mellitus has emerged as a global health crisis, primarily due to alterations in lifestyle and genetic factors. By 2030, it is estimated that around 438 million individuals will be impacted by type 2 diabetes. Metformin hydrochloride (MTH) is the most commonly prescribed antidiabetic worldwide for type 2 diabetes mellitus, as it effectively reduces blood glucose levels and is safe, readily accessible, and cost-effective [1, 2]. Metformin lowers basal and postprandial plasma glucose levels, thereby improving glucose tolerance in patients with type 2 diabetes. Metformin does not result in hyperinsulinemia or hypoglycemia in individuals with type 2 diabetes or healthy individuals, in contrast to sulfonylureas. Due to its short half-life of 1.5–4.5 hours and 50–60% bioavailability, MTH is an effective antidiabetic that requires regulated release [3, 4]. Thus, MTH is an ideal drug for a sustained-release drug delivery system, as a single dose of metformin provides up to 12 hours of therapeutic action.

A very effective sustained-release delivery for altering drug administration, based on the matrix material's composition, is anticipated to be constructed from naturally occurring polymers capable of forming hydrogel beads or microspheres. Interpenetrating polymer network (IPN) beads or microspheres are composed of at least two polymers that may crosslink to form a three-dimensional framework, creating void spaces for drug encapsulation [5–10]. Recent advancements highlight their critical role as drug-delivery machines, given their size and controlled-release properties. These structures also provide excellent conditions for extended drug release. Additionally, they are biocompatible and suitable for a wide range of molecules, including peptides, proteins, NSAIDs, and novel nanostructures [11–14]. Recent studies explore the functional properties of these materials across various biomedical applications. When a hydrophilic polymer chain penetrates a separate polymer blend without chemical bonding between them, a semi-IPN is formed. In a semi-IPN, only one network is crosslinked, whereas in an IPN, multiple crosslinked networks interpenetrate each other.

Gelatin (GE) is a biocompatible, biodegradable, and non-toxic natural polymer widely used in the formulation of controlled-release systems. Cross-linking methods are crucial for stabilizing gelatin structures for biomedical applications, influencing degradation kinetics and mechanical properties [15-18]. It is commonly employed for microencapsulation and enhances macrophage phagocytosis. GE microspheres are prepared by glutaraldehyde cross-linking to serve as controlled-release vesicles for targeting interferon delivery to macrophages. These microspheres have been proposed for the treatment of various diseases that require targeted drug concentration, either within the bloodstream or in specific cells or organs [19]. Hydroxyethyl cellulose (HEC) is a non-ionic polymer soluble in water. Due to its excellent functional properties, it is used for emulsification, thickening, binding, suspending, stabilizing, and dispensing. It also provides effective protective action. Additionally, HEC can be combined with gelatin to reduce pH-related reactions in the gastrointestinal tract [20-23].

IPN and semi-IPN structures in the context of drug delivery are extensively covered in the literature. Previous studies have developed various formulations based on IPNs as controlled-release drug delivery systems. For example, gelatin/sodium carboxymethyl cellulose semi-IPN microspheres containing ketorolac tromethamine were successfully prepared using glutaraldehyde(GA) as a crosslinking agent [24,25]. Kozlowska et al. formulated a collagen/gelatin/hydroxyethyl cellulose matrix incorporating 3% gellan gum microspheres produced by the emulsion technique [26]. Taboun A et al. demonstrated that gelatin type B, cross-linked with citric acid and strengthened with hydroxyapatite (HAp) and β-tricalcium phosphate particles, exhibits improved microhardness, presenting a promising new material with potential applications in dentistry [27].

Semi-IPN microbeads composed of modified karaya gum and sodium alginate, produced via traditional ionotropic gelation, have demonstrated potential as an effective delivery system for D-penicillamine [28]. Additionally, Hadke Jayshri and Khan Shagufta formulated a novel gastroretentive microsphere system based on *Sterculia foetida* and pullulan gum, optimized using a central composite design and fabricated via emulsion crosslinking [29].

However, published research specifically detailing the systematic optimization of a GE–HEC semi-IPN microsphere system for the sustained delivery of highly water-soluble MTH using a central composite design remains limited. Design of experiments (DoE) approaches are now widely used in pharmaceutical development to optimize formulations and processes [30]. This research focuses on the development and optimization of GE–HEC semi-interpenetrating polymer network (semi-IPN) microspheres for the sustained delivery of MTH

using a water-in-oil emulsion crosslinking technique. A central composite design (CCD) was employed to systematically investigate the effects of GE, HEC, and GA concentrations on key parameters, including drug entrapment efficiency, cumulative drug release, and particle size. The optimized formulation was comprehensively characterized using Fourier transform infrared spectroscopy (FTIR), differential scanning calorimetry (DSC), scanning electron microscopy (SEM), and in-vitro release studies. Particular emphasis was placed on elucidating the drug-release mechanism and assessing the formulation's potential for clinical diabetes management.

2. Materials and Methods

Metformin hydrochloride was provided by Hetero Laboratories Ltd., Hyderabad. GE, HEC, GA, Span 80, and light liquid paraffin were supplied by Scientific Chemicals. Analytical-grade chemicals were used throughout the study.

2.1. Formulation of semi-IPN microspheres.

Semi-IPN microspheres were formulated using the water-in-oil (w/o) emulsion cross-linking technique. A 20 ml polymer solution was prepared by mixing 14% w/w GE and HEC in distilled water, using a magnetic stirrer at 500 rpm and 37°C. MTH was weighed and added to the polymer solution, then stirred until a homogeneous dispersion was obtained. Using a homogenizer, the dispersion was gradually incorporated into 100 ml of light liquid paraffin containing 1% (w/v) Span 80, and stirred at 400 rpm for 10 minutes. After forming a milky white emulsion, glutaraldehyde solution (4.24% v/v) was added dropwise to the emulsion under continuous magnetic stirring at room temperature (25°C). The cross-linking reaction was allowed to proceed for a duration of 24 hours to ensure adequate stabilization of the polymeric network [29]. The microspheres were separated by filtration, and excess oil was removed by washing with n-hexane. Unreacted GA was removed by washing with 0.1 M glycine solution. The microspheres were then air-dried at 40°C for two days and stored in a desiccator for future use [31].

2.2. Experimental design.

2.2.1. Rationale for CCD variable ranges.

The ranges for the independent variables (GE, HEC, and GA) in the Central Composite Design were determined based on preliminary experiments and a review of relevant literature [32,33]. The concentration of GE (% w/v) was chosen to ensure adequate polymer viscosity for semi-IPN microspheres formation without causing excessive clumping. The HEC concentration (% w/v) was selected to provide an optimal balance of polymer properties for sustained release [34]. The GA volume (ml) was selected to achieve sufficient cross-linking for network stability without leading to an overly rigid structure that would hinder drug entrapment or result in excessive unreacted glutaraldehyde [35,36]. The application of systematic Design of Experiments (DoE) techniques in this manner is a widely established methodology in pharmaceutical product development to optimize complex formulations [37].

Semi-IPN microspheres were developed and optimized by manipulating three formulation variables. A central composite design with two levels was utilized to assess the influence of these formulation parameters. Specifically, varying quantities of GE (A), HEC

(B), and GA (C) were employed at two distinct levels, as detailed in Table 1, to prepare semi-IPN microspheres encapsulating MTH. The experimental design was constructed and analyzed using a trial version of Design-Expert® 11 software (Stat-Ease Inc., USA). The formulation variables hypothesized to affect the dependent responses in the design matrix included drug entrapment efficiency (DEE) (R1), cumulative percentage drug release (%CDR) after 12 hours (R2), and particle size (R3) [19]. To optimize the experimental design, the relationships between the independent variables and the dependent responses were modeled using a quadratic equation, as shown below.

$$R = \beta_0 + \beta_1 A + \beta_2 B + \beta_3 C + \beta_{\{12\}AB} + \beta_{\{13\}AC} + \beta_{\{23\}BC} + \beta^2_{\{11\}A} + \beta^2_{\{22\}B} + \beta^2_{\{33\}C} \quad (1)$$

The independent formulation variables are A, B, and C, and R is the measured response. b0 is the intercept.

Table 1. Formulation table for semi-IPN blend microspheres.

Formulation code	GE (%w/v): A	HEC (%w/v):B	GA (%v/v): C
F1	70	30	4.5
F2	70	30	0.295518
F3	53.1821	30	4.5
F4	60	40	2
F5	70	30	4.5
F6	70	30	8.70448
F7	60	20	2
F8	70	46.8179	4.5
F9	60	20	7
F10	70	30	4.5
F11	80	40	2
F12	70	13.1821	4.5
F13	80	20	2
F14	60	40	7
F15	70	30	4.5
F16	80	40	7
F17	70	30	4.5
F18	70	30	4.5
F19	86.8179	30	4.5
F20	80	20	7

2.2.2. Justification of parameter ranges.

The ranges for the independent variables (GE, HEC, and GA concentrations) were determined based on preliminary experimental studies and existing literature. Gelatin concentrations below 50% w/v resulted in microspheres with poor structural integrity, whereas concentrations above 87% w/v produced highly viscous solutions that were difficult to process via the emulsion crosslinking technique. Similarly, the HEC concentration range was selected to ensure adequate matrix formation while maintaining the necessary hydrophilicity for drug release. Glutaraldehyde concentrations were carefully selected to achieve sufficient cross-linking for sustained release without compromising the biocompatibility of the final formulation [21].

2.3. Evaluation of semi-IPN blends microspheres.

All evaluation parameters and subsequent analyses were performed in triplicate ($n = 3$), and results are expressed as mean± standard deviation (mean ±SD).

2.3.1. Drug entrapment efficiency.

10 mg of semi-IPN microspheres were ground to a fine powder using a mortar and pestle, then dispersed in 50 ml of deionized water and sonicated for 30 minutes. To thoroughly extract the drug, the solution was rinsed twice and centrifuged to remove polymeric debris. The clear supernatant was analyzed using a UV spectrophotometer set at 231 nm [31].

2.3.2. Particle size determination.

The particle size of the optimized formulation of semi-IPN microspheres was determined using the sieve analysis method. A mechanical sieve shaker equipped with standard sieves of mesh sizes #12, #14, #16, #18, and #22 was used to sieve accurately measured microspheres for 10 minutes, separating them into various sizes (based on their percentage fraction). The mean particle size (d) was calculated three times using the appropriate formula.

$$\text{Mean particle size} = \{\sum(P_f \times W_f)\}/\{\sum W_f\}$$

Where P_f stands for mean particle size, and W_f stands for weight fraction.

2.3.3. *In-vitro* drug release studies.

The USP Type II dissolution apparatus (Electro Lab India DS 8000) was employed to study drug release from the optimized semi-IPN microsphere formulation and other formulations under sink conditions. Each semi-IPN microsphere formulation, containing 10 mg of MTH, was accurately weighed and enclosed in muslin cloth. The cloth was securely attached to the paddle, and 900 mL of phosphate buffer (pH 6.4) was added. Drug release was monitored at 50 rotations per minute while maintaining the temperature at 37 ± 0.5°C. At 0.5, 1, 2, 4, 6, 8, 10, and 12-hour intervals, 5 mL samples were withdrawn and immediately replaced with fresh dissolution medium. The results represent the average of three determinations.

2.3.4. Statistical analysis.

The formulations were statistically optimized using a trial version of Design-Expert® 11 software (Stat-Ease Inc., USA). The mean and standard deviation represent the results of individual measurements, each performed in triplicate (n = 3). An ANOVA was conducted for each dependent parameter to evaluate the effect of each independent variable or factor selected for this study, based on the probability value (p-value). A response factor was considered statistically significant if its p-value was less than 0.05; conversely, a response term was deemed insignificant if its p-value exceeded 0.05. Additionally, the F-test and p-values were generated by the software.

It was possible to better understand the relationships among factors and responses by using response surface, contour, and perturbation plots. Perturbation plots illustrate the deviation of the response from its nominal value when all other parameters are held constant at a reference point. The curvature or steepest slope indicates sensitivity to specific factors. Response surface and contour plots were analyzed to understand how these variables and their interactions influenced the responses.

2.3.4.1. Model validation and adequacy.

The adequacy of the quadratic models generated by the software was assessed using standard statistical metrics, including the adjusted R^2 (R^2 adj) and predicted R^2 (Pred-R^2). These metrics were used to confirm that the models could reliably predict experimental outcomes. Furthermore, a lack-of-fit test was performed for each model; a non-significant *p*-value ($p > 0.05$) in this test confirmed the model's appropriateness for the experimental data.

2.3.5. Numerical optimization.

To develop an optimized procedure that achieves the desired results, both numerical and graphical optimization techniques were employed. Using software, multiple responses were simultaneously optimized after appropriate models for each response were established and statistically analyzed. The objective was to identify a set of factor values that simultaneously satisfied the criteria for all responses.

Software can identify which design elements are most likely to impact the system using this strategy positively. The anticipated response values were calculated using ramp solutions, an optimized formulation, and a desirability plot developed under new, improved conditions. The software's robustness and the percentage of projected error were assessed by comparing the experimental response values generated by the optimized formulation with the software's predicted values. To ensure the results fall within an acceptable range, the expected error must be less than 15%.

2.3.6. Characterization of optimized formulation.

2.3.6.1. FTIR studies.

To assess the drug's stability within the polymeric matrix, the FTIR spectra of the pure active pharmaceutical ingredient, MTH, and the optimized semi-IPN microsphere formulation were analyzed. Samples (2 mg) were compressed with potassium bromide (200 mg) into KBr pellets using a hydraulic press. Each KBr pellet was scanned over a wave number range of 500 to 4000 cm^{-1}. Distinct bands were observed in both samples.

2.3.6.2. DSC study.

The differential scanning calorimetry study was conducted using a TA Instruments Model SDT Q600 thermal analysis system. The samples were heated at 10°C/min from 50 to 300°C under an inert nitrogen atmosphere to control the endothermic melting temperatures of the pure drug MTH and the optimized semi-IPN microsphere formulation.

2.3.6.3. Scanning electron microscopy (SEM) study.

The best formulation of semi-IPN blend microspheres of MTH surface morphology was examined and recorded using a Zeiss scanning electron microscope. The gold coating was sputtered onto microspheres on a copper stub under high vacuum to create thin gold coatings [21].

2.3.6.4. Release kinetics.

The release kinetics of the optimized formulation were studied using various kinetic models, including zero-order, first-order, Higuchi, and Korsmeyer-Peppas models, to fit the *in vitro* drug release data [31].

2.3.6.5. Stability studies.

In accordance with ICH guidelines, stability testing of the optimized formulation was conducted over six months. The study utilized a stability chamber maintained at 40°C ± 2°C and 75% ± 5% RH, with the formulation wrapped in laminated aluminum foil. Samples were evaluated after one, three, and six months to assess significant changes in drug entrapment efficiency (DEE), particle size, and percentage cumulative drug release (%CDR) at the 12th hour [38-40].

3. Results and Discussion

In the current study, sustained drug release of MTH was achieved by developing semi-IPN microspheres composed of GE and HEC, with MTH incorporated and GA used as a cross-linking agent. To modify the amine groups, a trace amount of GA was removed from the microspheres during manufacturing by periodically washing them with 0.1 M glycine solution. This washing facilitated the formation of imine bonds through a reaction with the deactivated glutaraldehyde groups of unreacted GA, effectively eliminating residual glutaraldehyde introduced during formulation. Brady's test confirmed the absence of GA in the optimized formulations, indicating their suitability for various applications.

3.1. Influence of drug entrapment efficiency (R1).

As the polymer concentration increases, the percentage of DEE rises from 60.97 ± 1.95% to 77.98 ± 1.46%, as shown in Table 2. Figures 1a, 1b, and 1c use perturbation plots and 2D and 3D response surface plots to illustrate how various factors influence drug encapsulation efficiency (DEE). The response surface plot shows that increasing the gelatin concentration increases the drug encapsulation efficiency to an optimal level. The following polynomial equation relates DEE to the independent variables.

$$R_1 = +74.40 + 0.1014\,A + 1.64\,B + 2.91\,C - 0.0763\,AB - 0.8187\,AC + 0.6788\,BC - 2.58\,A^2 + 0.0476\,B^2 - 3.63\,C^2 \quad (2)$$

Table 2. Design an expert matrix of formulations along with factors and their responses.

Formulation Code	A: GE(%W/V)	B: HEC(%W/V)	C: GA(%V/V)	R1: (DEE) (%) (Mean±S.D), n=3	R2: (CDR at 12h) (%) (Mean±S.D), n=3	R3: (Particle Size) (µm) (Mean±S.D), n=3
F1	70	30	4.5	74.17±0.35	76.89±0.82	140±2.1
F2	70	30	0.295518	61.8±0.54	72.44±0.65	112±1.5
F3	53.1821	30	4.5	72.14±0.41	69.77±1.05	86±1.2
F4	60	40	2	61.76±0.29	67.8±0.93	118±1.8
F5	70	30	4.5	73.8±0.38	75.69±0.77	136±2.0
F6	70	30	8.70448	69.82±0.47	62.34±1.22	117±1.4
F7	60	20	2	60.97±0.31	59.66±0.88	108±1.1
F8	70	46.8179	4.5	77.98±0.52	67.37±1.01	114±1.9
F9	60	20	7	65.71±0.39	59.22±0.74	121±2.2
F10	70	30	4.5	74.1±0.36	74.98±0.81	136±1.7
F11	80	40	2	68.53±0.45	65.28±0.95	111±1.3
F12	70	13.1821	4.5	74.45±0.42	70.96±0.86	109±1.6

Formulation Code	A: GE(%W/V)	B: HEC(%W/V)	C: GA(%V/V)	R1: (DEE) (%) (Mean±S.D), n=3	R2: (CDR at 12h) (%) (Mean±S.D), n=3	R3: (Particle Size) (µm) (Mean±S.D), n=3
F13	80	20	2	63.81±0.33	52.8±0.69	112±1.5
F14	60	40	7	73.45±0.48	59.54±1.03	99±1.4
F15	70	30	4.5	74.56±0.37	75.78±0.79	136±1.8
F16	80	40	7	72.71±0.51	77.75±1.21	97±1.2
F17	70	30	4.5	74.88±0.40	74.98±0.84	139±2.3
F18	70	30	4.5	74.34±0.39	75.65±0.80	136±1.9
F19	86.8179	30	4.5	65.43±0.44	73.67±0.98	93±1.1
F20	80	20	7	69.51±0.49	76.62±1.07	115±1.6

A: Gelatin; B: Hydroxy ethylcellulose; C: Glutaraldehyde; R1:DEE: Drug Entrapment Efficiency; R2:CDR: Cumulative drug release; R3:Particle size.

Where B is the volume of HEC (% w/v), C is the volume of glutaraldehyde (ml), and A is the quantity of gelatin (% w/v). An excellent fit was observed in the central composite design. The model was significant, as indicated by a model F-value of 5.52 and a p-value less than 0.05. However, the negative predicted R^2 (-0.4411) suggests that the overall mean may be a better predictor of the response than the model for predictive purposes outside the tested range. The signal-to-noise ratio, measured by adequate precision, was 8.694, exceeding the preferred threshold of 4. This indicates an adequate signal, meaning the model can be used to explore the design space and identify significant factor trends. The lack-of-fit F-value of 120.24 indicates a significant lack of fit. In the polynomial equation (2), terms C, A^2, and C^2 are significant, as their p-values are less than 0.05.

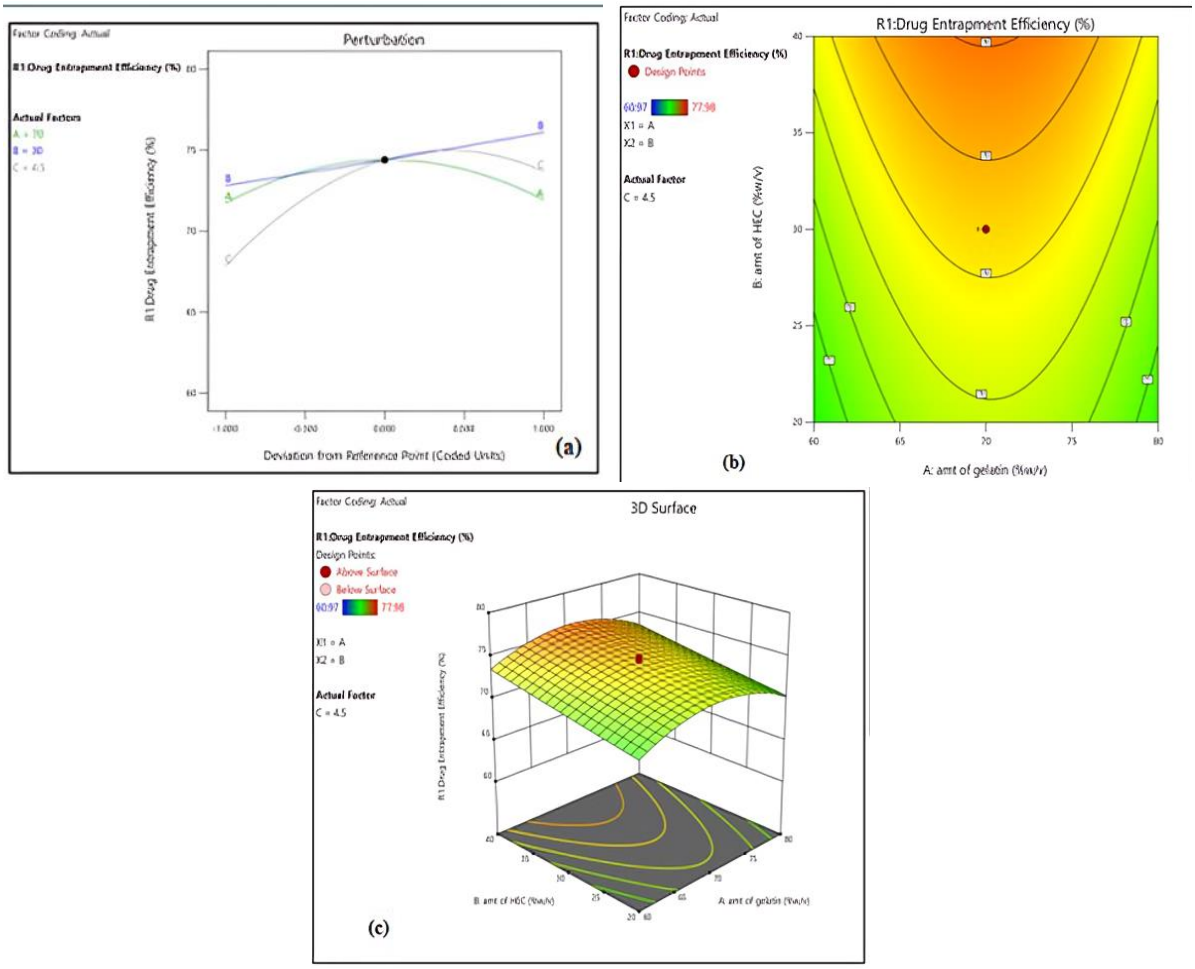

Figure 1. (a) Perturbation plot; **(b)** 2D-response surface plot; **(c)** 3D-response surface plot showing the influence of factors (A: amount of gelatin (%w/v), B: amount of HEC, and C: volume of glutaraldehyde (ml) on drug entrapment efficiency (%DEE).

Figure 1(a), 1(b), and 1(c) utilize perturbation plots as well as 2D and 3D response surface plots to illustrate how various factors influence the drug encapsulation efficiency (DEE). The perturbation plots reveal that GE concentration (factor A), which was found to have a significant effect on DEE, increases DEE. Conversely, the nonlinear effects of the squared terms of factors A and C are indicated by slight curvilinear trends, suggesting that higher levels of A^2 and C^2 correspond to lower DEE values. Additionally, it was determined that the concentration of hydroxyethyl cellulose (HEC), or factor B, has no significant impact on DEE, as indicated by the p-value analysis.

Although the composition of GA (C) was maintained constant at 4.5 ml, the curvature effects of DEE concentration on GE (A) and HEC (B) were illustrated using 2D and 3D response surface plots. DEE initially increases and then decreases at low concentrations of HEC (B) as the amount of gelatin (A) rises to an intermediate level. Therefore, it was concluded that A and B exert a parabolic influence on DEE due to a significant interaction effect ($p<0.05$ for AB term in the ANOVA).

Thus, it was evident that the high viscosity of the polymer mixtures and the increased GE (A) levels contributed to the rise in DEE, thereby reducing drug leakage during microsphere formation. Moreover, the higher drug entrapment within the semi-IPN network likely resulted from the increased polymer concentration, reaching the optimized level. However, as the GA volume increases, encapsulation efficiency decreases; this decline may be attributed to a higher density of cross-linking, which rapidly forms a rigid structure during the manufacturing process, physically impeding optimal drug partitioning and entrapment within the polymer network before solidification.

3.2. Influence of formulation factors on % CDR (R2).

All batches of semi-IPN microspheres exhibited a cumulative drug release (% CDR) ranging from 52.8% to 77.75%, as shown in Table 2. The following polynomial equation describes the relationship between the factors and the responses.

$$R_2 = +75.80 + 2.40\,A + 1.17\,B + 0.7765\,C + 0.6438\,AB + 5.62\,AC - 2.40\,BC - 2.28\,A^2 - 3.19\,B^2 - 3.81\,C^2 \quad (3)$$

A p-value of less than 0.05 and an F-value of 3.28 indicate that the model is statistically significant for identifying the influence of the factor. The variance is greater than 0.2; however, the predicted R^2 of -0.9094 is not as close to the adjusted R^2 of 0.5187 as typically expected, suggesting limitations in the model's predictive accuracy. In this context, accuracy represents the signal-to-noise ratio, with an ideal value greater than 4. The program produced an adequate accuracy ratio of 5.110, suggesting a sufficient signal to justify using the quadratic model to explore the design space for trend analysis. The lack of fit is significant, as indicated by the lack of fit F-value of 105.81. At a significance level of 0.05, the model terms AC, B^2, and C^2 are considered significant based on their p-values in the polynomial equation above.

Factors B and C were shown to have a substantial influence on the percentage CDR at 12 hours, as demonstrated by perturbation plots. The nonlinear effect of the squared terms of B and C is indicated by a slight curvature in the plots. Consequently, higher levels of B^2 and C^2 correspond to lower CDR values. It was also found that factor A, representing the concentration of GE, had no discernible impact on the overall CDR rate.

The contour and response surface plots shown in Figures 2a, 2b, and 2c illustrate the effects of factors A and B on the percentage of cumulative drug release (% CDR). The plots indicate that, from low to high levels of factor B (HEC), the drug release rate decreases, suggesting a controlled release of MTH. This effect is notably enhanced when factor C (GA) is held constant at higher levels, showing a clear interaction between HEC concentration and the degree of cross-linking. This phenomenon is attributed to the formation of a more rigid and denser polymer matrix surrounding the drug. The increased cross-linking density physically impedes the diffusion of MTH molecules through the network, thereby facilitating sustained drug delivery.

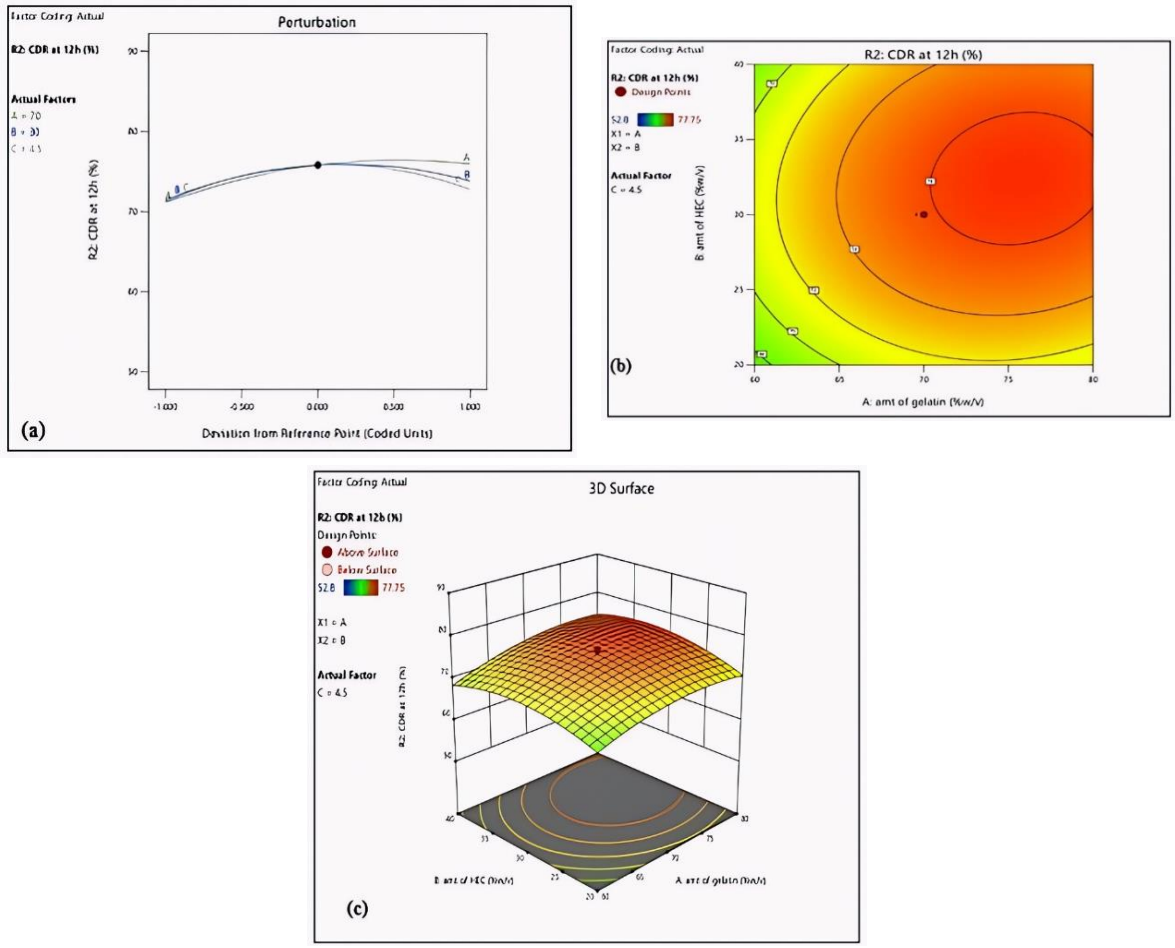

Figure 2. (a) Perturbation plot; **(b)** 2D-response surface plot; **(c)** 3D-response surface plot showing the influence of factors (A: amount of gelatin (%w/v), B: amount of HEC, and C is the volume of glutaraldehyde (ml) on CDR at 12 h.

3.3. Influence of particle size (R3).

All batches of particle diameters in semi-IPN microspheres ranged from 86 to 140 µm, as shown in Table 2. Figures 3a, 3b, and 3c employ perturbation plots, along with 2D and 3D response surface plots, to demonstrate how various factors influence particle size. The following polynomial equation describes the relationship between the factors and the responses.

$$R_3 = +136.94 + 0.0566\,A - 1.65\,B - 0.6291\,C - 0.8750\,AB - 0.6250\,AC - 6.13\,BC - 15.40\,A^2 - 7.62\,B^2 + 6.56\,C^2 \quad (4)$$

The model's p-value was less than 0.05, indicating that the model is statistically significant, as supported by the model's F-value of 13.64. Although the adjusted R^2 of 0.8568 and the predicted R^2 of 0.4411 are not closely aligned—the difference exceeds 0.2—the signal-to-noise ratio demonstrates sufficient precision. Ideally, this ratio should be greater than 4; here, the value of 10.078 suggests a strong signal for analyzing factor effects on particle size.

The contour and response surface plots (Figures 3a, 3b, 3c) illustrate significant interaction effects, particularly the strong negative relationship between HEC (B) and GA volume (C) as indicated by the prominent 'BC' term in the equation. Higher concentrations of these components interact to reduce overall particle size, likely due to increased cross-linking density, leading to denser, more compact microspheres during formation. Higher concentrations of these components interact to reduce overall particle size, likely due to increased cross-linking density, leading to denser, more compact microspheres during formation. However, the lack-of-fit F-value of 21.28 indicates a significant lack of fit. At a significance level of 0.05, the polynomial terms BC, A^2, B^2, and C^2 are identified as significant contributors to the model.

Figures 3a, 3b, and 3c employ perturbation plots, along with 2D and 3D response surface plots, to demonstrate how various factors influence particle size. The perturbation plots highlight the significant effects of the squared terms for factors A, B, and C, as well as the interaction between factors B and C, indicated by a steep decrease in particle size. Additionally, particle size is independently affected by other formulation parameters, as evidenced by the R^2 value.

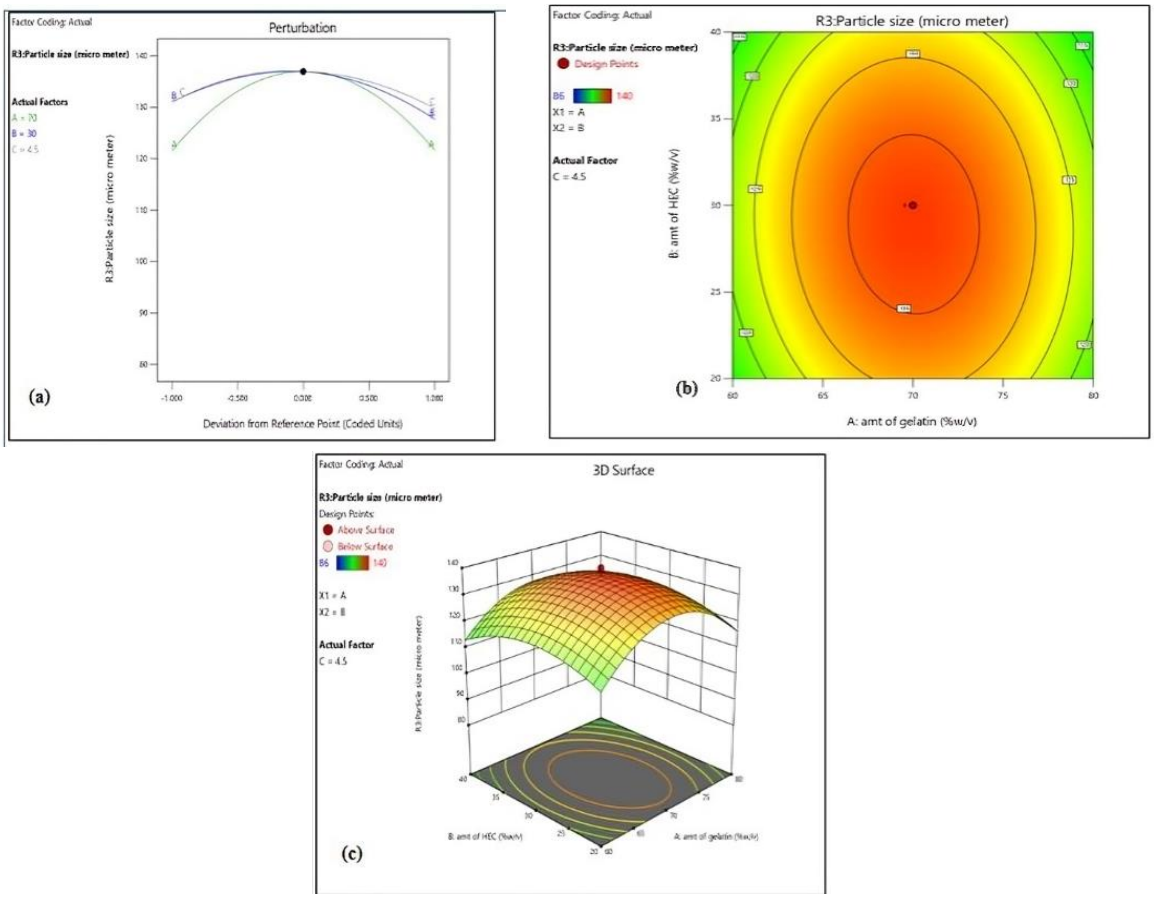

Figure 3. (a) Perturbation plot; **(b)** 2D-response surface plot; **(c)** 3D-response surface plot showing the influence of factors (A: amount of gelatin (%w/v), B: amount of HEC, and C: volume of glutaraldehyde (ml) on particle size.

The curvature effects of GE (A) and HEC (B) concentrations on particle size were illustrated using 2D and 3D response surface plots, with the GA (C) concentration held constant at 4.5 ml. A decrease in viscosity at low concentrations of HEC (B) and GE (A) leads to a reduction in particle size. Conversely, particle size increases with the squared effects of A and B but decreases when factor B increases and component A decreases. The 3D response surface plots exhibited similar trends.

The increase in particle size may be attributed to higher concentrations of GE, HEC, and GA, which promote the formation of larger secondary microparticles. The model terms BC, A^2, B^2, and C^2 have been identified as significant contributors.

3.4. Optimization by desirability function.

The desirability function served as the basis for the optimization process. Microspheres were prepared under the optimal conditions predicted by the model generated by the software, using 66.2568% w/v GE, 22.9008% w/v HEC, and 3.39903 ml GA, as shown in Table 3 and represented as F21. The dependent variables were constrained at 12 hours to 70.9345% for DEE (R1), 71.4075% for CDR, and 128.855 µm for particle size to facilitate optimization, as illustrated in Figure 4 (Overlay plot). The model's reliability was confirmed by the response variables for microspheres formed under optimal conditions, which showed minimal percentage bias relative to the predicted values, indicating the reproducibility of the optimized formulation F21 within acceptable experimental error.

Table 3. Confirmation of the dependability of the model in optimal conditions.

Optimized formulation	Optimum conditions			Responses	Predicted value (PV)	Experimental value (EV) (n=3)	Bias (%) = (PV-EV)/PV*100
	A (%w/v)	B (%w/v)	C (ml)				
F21	79.85	26.98	4.24	R1	72.3	68.4±1.15	5.39
				R2	73.6	70.7±0.92	3.94
				R3	134.62	126.8±2.45	5.80

PV: Predicted value generated by Design-Expert software based on a quadratic model.

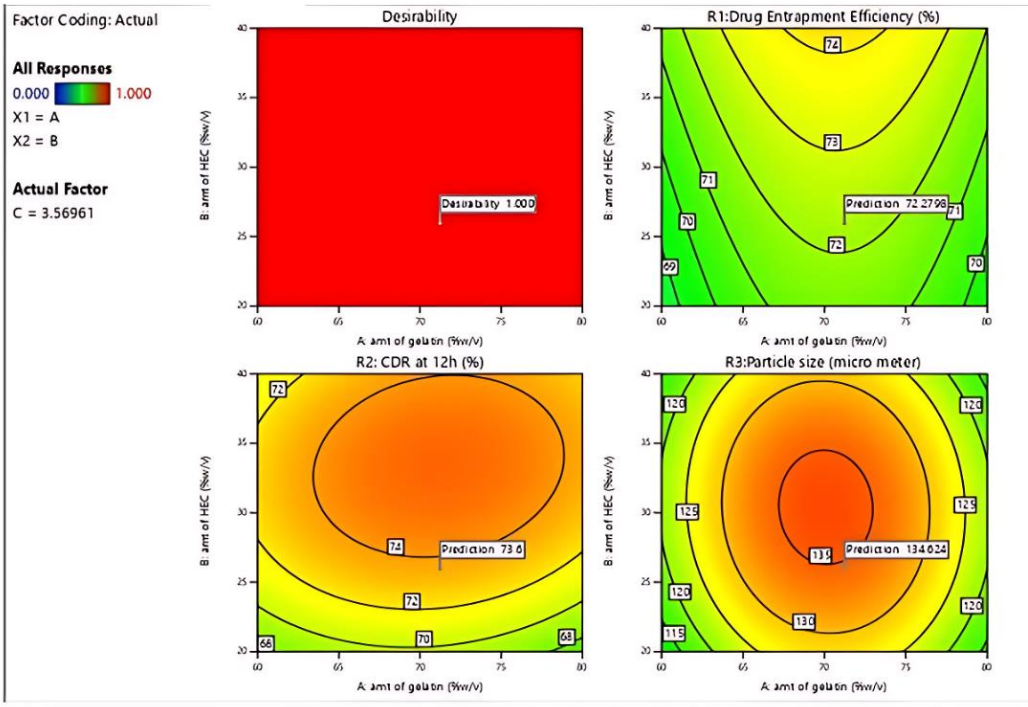

Figure 4. Desirability plot.

3.5. Characterization of semi-IPN microspheres.

3.5.1. FTIR study.

The FTIR spectra of pure MTH and the optimized formulation were analyzed (Figure 5(a) and 5(b)). The pure MTH spectrum (Figure 5(a)) showed characteristic peaks at 3433.04 cm^{-1} and 3551.90 cm^{-1} (assigned to N-H stretching bands) and 1635.52 cm^{-1} (assigned to C=N stretching or N-H bending). Other notable bands appeared in the 2842–2468 cm^{-1} range and the fingerprint region (1498–580 cm^{-1}).

The FTIR spectrum of the optimized formulation (Figure 5(b)) exhibited a broad O-H/N-H stretching band centered around 3433.04 cm^{-1}. In the optimized formulation's spectrum, the sharp characteristic N-H peaks of MTH at 3551.90 cm^{-1} are absent, merging into this broader polymeric peak. The C=N stretching peak in the formulation appeared around 1604.86 cm^{-1}, showing a minor shift compared to the pure MTH peak at 1635.52 cm^{-1}. This specific shift and the broadening of the O-H/N-H region indicate the presence of strong intermolecular hydrogen bonding interactions between the MTH molecules and the GE–HEC polymer matrix, confirming successful encapsulation and compatibility, which likely contributes to the sustained, non-Fickian release profile observed.

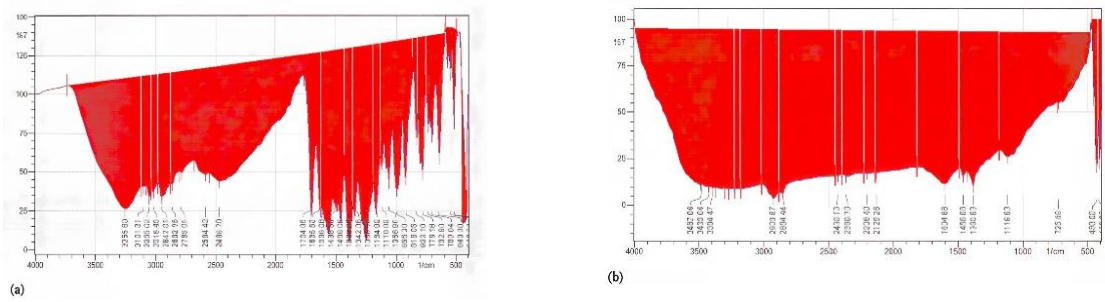

Figure 5. (a) FTIR spectra of drug (MTH); **(b)** FTIR spectra of optimized formulation (F21).

3.5.2. DSC study.

The DSC thermograms of pure API (MTH) and formulation F21 are shown in Figure 6 (a) and (b). The melting point of MTH is indicated by a strong endothermic peak on the thermogram of the pure API, observed at 214.6°C. The thermogram of F21 exhibits a distinct endothermic peak at 217.9°C. The minor upward shift in the melting point of MTH between the pure drug and F21 thermograms, coupled with the absence of additional peaks, suggests that the API is uniformly dispersed in the optimized formulation and has not undergone significant chemical interaction with the polymers that would alter its crystalline structure.

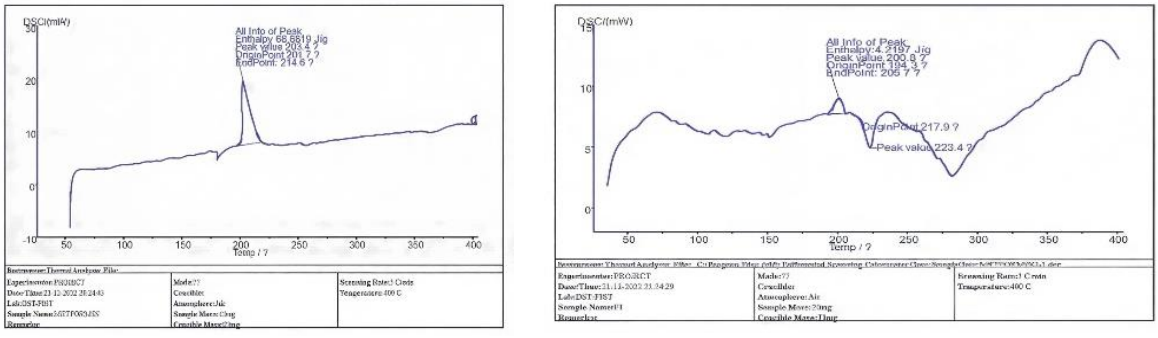

(a) **(b)**

Figure 6. (a) DSC thermogram of pure drug (MTH); **(b)** DSC thermogram of optimized formulation (F21).

3.5.3. SEM.

Scanning electron microscopy (SEM) was used to assess the surface morphology and particle size of the optimized formulation F21 (Figure 7). The images clearly show that the microspheres are predominantly spherical and monodisperse, with a rough surface texture characterized by tiny fissures. The average particle diameter observed via image analysis was approximately 126.8 ± 0.67 µm (consistent with sieve analysis results). The presence of a rough surface might influence the drug release profile by increasing surface area for dissolution, contributing to the initial drug release phase before the anomalous diffusion mechanism takes over.

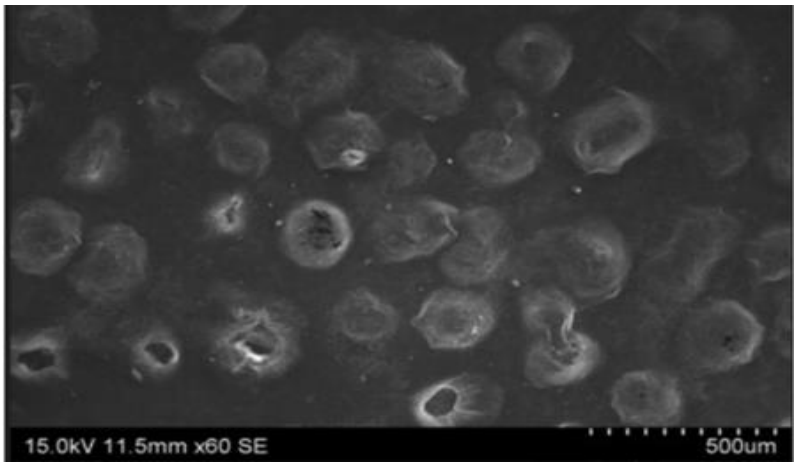

Figure 7. SEM photograph of optimized formulation (F21).

3.5.4. Release studies.

Using the Higuchi, Korsmeyer-Peppas, zero-order, and first-order models to correspond with in vitro drug release investigations, the release kinetics of the optimized formulation (F21) were determined and are shown in Table 4 and Figures 8(a), 8(b), 8(c), and 8(d). It was abundantly obvious from the data that the drug followed anomalous (non-Fickian) diffusion to exhibit first-order kinetics (R^2 = 0.981). By fitting the dissolution data, the drug release pattern follows first-order kinetics, indicating that GE-HEC semi-IPN microspheres contain water-soluble drugs in porous matrices. The proportionality of the amount of drug release from the polymer matrices by unit time diminishes along with non-swellable matrices, which are supported by an anomalous transport mechanism via Higuchi diffusion. The Korsmeyer-Peppas exponent (n) value of 0.714 is intermediate between 0.5 (Fickian diffusion control) and 1.0 (polymer relaxation/swelling control). This indicates anomalous transport, a complex mechanism in which the release rate is jointly controlled by the drug's diffusion through the porous matrix and the polymer network's swelling/degradation properties. This result revealed that the degradation properties of drug-encapsulated GE-HEC semi-IPN microspheres and the drug's diffusion jointly controlled (anomalous transport) the MTH release rates.

Table 4. Drug release kinetics of optimized formulation (F21).

Formulation code	Zero order	First order	Higuchi	Korsemeyer-Peppas model	
	R^2	R^2	R^2	N	R^2
F21	0.917	0.980	0.969	0.714	1.171

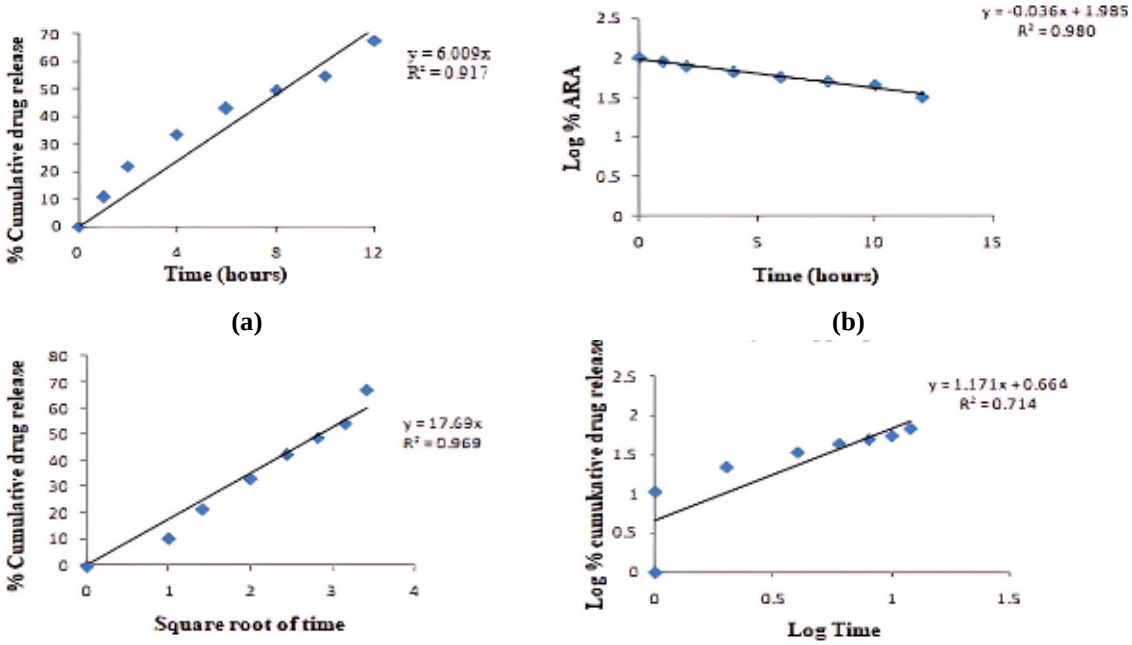

Figure 8. (a) Zero order; **(b)** First order; **(c)** Higuchi; **(d)** Korsmeyer Peppas plot for optimized formulation F21.

3.5.5. Comparison with published metformin microspheres studies.

For contextual comparison, the F21 formulation was benchmarked against general findings in metformin microsphere research, as shown in Table 5. This analysis helps position our results relative to those published in the scientific literature.

Table 5. Comparison of F21 formulation characteristics with published metformin microsphere studies.

Formulation/ Study	Polymer(s) Used	Preparation Method	Release Exponent (n)	Dominant Release Mechanism	Metformin Release Profile	Reference
F21 (Current Study)	GE-HEC semi-IPN	N/A	0.714	Anomalous Transport	First-order sustained release	(This study)
Example Study A	Alginate/Chitosan	Ionotropic Gelation	~0.53	Fickian Diffusion	Sustained (12 hrs)	[41]
Example Study B	Eudragit RS100	Solvent Evaporation	~0.95	Case-II Transport	Extended Release	[42]
Example Study C	HPMC/ Carbopol	N/A	~0.61	Anomalous Transport	Sustained Release (8 hrs)	[43]

3.5.6. Stability studies.

After exposure to accelerated temperature and humidity conditions for three months, the optimized formulation (F21) was determined to be stable. This conclusion is based on stability studies conducted under accelerated conditions, assessing %DEE, %CDR at 12 hours, and particle size, as shown in Table 6.

Table 6. Stability studies data for optimized formulation (F21).

Dependent factors	0 month	I month	II month	III month
% Drug entrapment efficacy (DEE)	68.4±0.99	66.2±1.20	65.4±1.12	64.8±0.92
%CDR at 20 out of 12h	70.7±1.23	68.7±0.79	67.4±0.88	67.7±1.03
Particle size (µm)	126.8±0.67	124.8±0.72	125.2±1.90	123.8±1.11

No 'significant change' was observed in any of the parameters characterized for the F21 formulation over the three-month period, as assessed against the criteria specified in ICH Q1A

guidelines (e.g., typically a maximum 5% deviation in assay is acceptable within limits), confirming the robustness and integrity of the formulation.

4. Conclusion

Semi-IPN microspheres encapsulating MTH were successfully developed and optimized using a water-in-oil emulsion cross-linking method, employing glutaraldehyde (GA) as the cross-linking agent and gelatin (GE) and hydroxyethyl cellulose (HEC) as polymer components. Under optimized conditions, formulation F21 was prepared, containing approximately 66.26% w/v GE, 22.90% w/v HEC, and 3.40 ml glutaraldehyde. This optimized formulation, which achieved a drug entrapment efficiency (DEE) of 68.4±0.99%, a cumulative drug release of 70.7±1.23% over 12 hours, and a particle size of 126.8±0.67 µm, exhibited values that closely matched those predicted by computational modeling, with minimal percentage bias. DSC and FTIR analyses confirmed uniform drug dispersion within the polymer matrix and favorable drug-polymer compatibility. SEM studies revealed that the microspheres had a spherical morphology with a predominantly rough surface characterized by fine fissures. Drug release kinetics followed a first-order model, governed by a combination of diffusion and matrix erosion mechanisms (anomalous transport). The optimized formulation (F21) demonstrated sustained drug release profiles and stability under the evaluated accelerated conditions. The GE–HEC semi-IPN microspheres platform offers an economical, biocompatible, and scalable approach for the development of sustained-release oral drug delivery systems. The use of a standard water-in-oil emulsion method facilitates potential industrial scaling. Future research should prioritize in vivo pharmacokinetic and pharmacodynamic studies to validate the sustained-release properties and therapeutic efficacy observed in vitro.

Author Contributions

Conceptualization, J.D.; methodology, A.G., S.M., and P.A.; software, A.G. and S.S.R.; validation, J.D. and A.G.; formal analysis, A.G., S.M., and S.S.; investigation, J.D., A.G., S.M., P.A., S.S.R., S.T., and S.S.; resources, J.D.; data curation, A.G. and S.M.; writing—original draft preparation, J. D., A.G. and S.M.; writing—review and editing, J.D.; visualization, A.G. and S.T.; supervision, J.D.; project administration, J.D.
All authors have read and agreed to the published version of the manuscript.

Institutional Review Board Statement

Not applicable.

Informed Consent Statement

Not applicable.

Data Availability Statement

Data supporting the findings of this study are available upon reasonable request from the corresponding author.

Funding

This research received no external funding.

Acknowledgments

We acknowledge Sri Krishnadevaraya University College of Pharmaceutical Sciences, S.K. University, for providing laboratory facilities.

Conflicts of Interest

The authors declare no conflict of interest.

References

1. Kotha, A.A.; Ahmad, S.U.; Dewan, I.; Bhuiyan, M.A.; Rahman, F.I.; Naina Mohamed, I.; Reza, M.S. Metformin Hydrochloride Loaded Mucoadhesive Microspheres and Nanoparticles for Anti-Hyperglycemic and Anticancer Effects Using Factorial Experimental Design. *Drug Des. Dev. Ther.* **2023**, *17*, 3661-3684, https://doi.org/10.2147/DDDT.S432790.
2. Laura, M.; Giuseppe, M.; Giona, C.; Luciano, B.; Maurizio, A.; Fabio, A.; Antonio, C.; Erika, C.; Maria Grazia, F.; Carmen, I.; Roberto, P.; Alberto, R.; Giuseppe, R.; Olga Eugenia, D. Improving Type 2 Diabetes Care with Extended-Release Metformin: Real-Life Insights from a Physician Educational Program. *Endocr. Metab. Immune Disord. Drug Targets* **2024**, *24*, 1422-1430, https://doi.org/10.2174/0118715303294909240221102552.
3. Asna Khalid, V.K.; Pillai, M.K. Design and statistical optimization of metformin hydrochloride loaded floating microspheres: influence of natural polymers. *Int. J. Pharm. Sci. Res.* **2023**, *14*, 5274-5280, https://doi.org/10.13040/IJPSR.0975-8232.
4. Alam, S.; Bishal, A.; Bandyopadhyay, B. Formulation and evaluation of metformin hydrochloride sustained release matrix tablets. *Int. J. Curr. Pharm. Res.* **2021**, *13*, 82-88, https://doi.org/10.22159/ijcpr.2021v13i5.1899.
5. Vashist, A.; Gupta, Y.K.; Ahmad, S. Interpenetrating biopolymer network based hydrogels for an effective drug delivery system. *Carbohydr. Polym.* **2012**, *87*, 1433-1439, https://doi.org/10.1016/j.carbpol.2011.09.030.
6. Zou, Z.; Zhang, B.; Nie, X.; Cheng, Y.; Hu, Z.; Liao, M.; Li, S. A sodium alginate-based sustained-release IPN hydrogel and its applications. *RSC Adv.* **2020**, *10*, 39722-39730, https://doi.org/10.1039/D0RA04316H.
7. Onugwu, A.L.; Nwagwu, C.S.; Onugwu, O.S.; Echezona, A.C.; Agbo, C.P.; Ihim, S.A.; Emeh, P.; Nnamani, P.O.; Attama, A.A.; Khutoryanskiy, V.V. Nanotechnology based drug delivery systems for the treatment of anterior segment eye diseases. *J. Control. Release* **2023**, *354*, 465-488, https://doi.org/10.1016/j.jconrel.2023.01.018.
8. Chen, H.; Regeard, C.; Salmi, H.; Morlet-Savary, F.; Giacoletto, N.; Nechab, M.; Xiao, P.; Dumur, F.; Lalevée, J. Interpenetrating polymer network hydrogels using natural based dyes initiating systems: Antibacterial activity and 3D/4D performance. *Eur. Polym. J.* **2022**, *166*, 111042, https://doi.org/10.1016/j.eurpolymj.2022.111042.
9. Lohani, A.; Singh, G.; Bhattacharya, S.S.; Verma, A. Interpenetrating Polymer Networks as Innovative Drug Delivery Systems. *J. Drug Deliv.* **2014**, *2014*, 583612, https://doi.org/10.1155/2014/583612.
10. Arafat, M.; Sarfraz, M.; Bostanudin, M.F.; Esmaeil, A.; Salam, A.; AbuRuz, S. In Vitro and In Vivo Evaluation of Oral Controlled Release Formulation of BCS Class I Drug Using Polymer Matrix System. *Pharmaceuticals* **2021**, *14*, 929, https://doi.org/10.3390/ph14090929.
11. Farasati Far, B.; Naimi-Jamal, M.R.; Safaei, M.; Zarei, K.; Moradi, M.; Yazdani Nezhad, H. A Review on Biomedical Application of Polysaccharide-Based Hydrogels with a Focus on Drug Delivery Systems. *Polymers* **2022**, *14*, 5432, https://doi.org/10.3390/polym14245432.
12. Ansari, M.J.; Rajendran, R.R.; Mohanto, S.; Agarwal, U.; Panda, K.; Dhotre, K.; Manne, R.; Deepak, A.; Zafar, A.; Yasir, M.; et al. Poly(*N*-isopropylacrylamide)-Based Hydrogels for Biomedical Applications: A Review of the State-of-the-Art. *Gels* **2022**, *8*, 454, https://doi.org/10.3390/gels8070454.

13. Li, T.; Lu, X.-M.; Zhang, M.-R.; Hu, K.; Li, Z. Peptide-based nanomaterials: Self-assembly, properties and applications. *Bioact. Mater.* **2022**, *11*, 268-282, https://doi.org/10.1016/j.bioactmat.2021.09.029.
14. Abdi, G.; Jain, M.; Patil, N.; Tariq, M.; Choudhary, S.; Kumar, P.; Raj, N.S.; Mohsen Ali, S.S.; Uthappa, U.T. Tragacanth gum-based hydrogels for drug delivery and tissue engineering applications. *Front. Mater.* **2024**, *11*, 1296399, https://doi.org/10.3389/fmats.2024.1296399.
15. Milano, F.; Masi, A.; Madaghiele, M.; Sannino, A.; Salvatore, L.; Gallo, N. Current Trends in Gelatin-Based Drug Delivery Systems. *Pharmaceutics* **2023**, *15*, 1499, https://doi.org/10.3390/pharmaceutics15051499.
16. Parente, J.F.; Sousa, V.I.; Marques, J.F.; Forte, M.A.; Tavares, C.J. Biodegradable Polymers for Microencapsulation Systems. *Adv. Polym. Technol.* **2022**, *2022*, 4640379, https://doi.org/10.1155/2022/4640379.
17. Rehman, U.; Sarfraz, R.M.; Mahmood, A.; Mahmood, T.; Batool, N.; Haroon, B.; Benguerba, Y. Tamarind/β-CD-g-poly (MAA) pH responsive hydrogels for controlled delivery of Capecitabine: fabrication, characterization, toxicological and pharmacokinetic evaluation. *J. Polym. Res.* **2022**, *30*, 41, https://doi.org/10.1007/s10965-022-03422-7.
18. Ruan, L.; Su, M.; Qin, X.; Ruan, Q.; Lang, W.; Wu, M.; Chen, Y.; Lv, Q. Progress in the application of sustained-release drug microspheres in tissue engineering. *Mater. Today Bio* **2022**, *16*, 100394, https://doi.org/10.1016/j.mtbio.2022.100394.
19. Zhou, H.Y.; Chen, X.G.; Liu, C.S.; Meng, X.H.; Yu, L.J.; Liu, X.Y.; Liu, N. Chitosan/Cellulose Acetate Microspheres Preparation and Ranitidine Release In Vitro. *Pharm. Dev. Technol.* **2005**, *10*, 219-225, https://doi.org/10.1081/pdt-54421.
20. Ashique, S.; Mishra, N.; Mohanto, S.; Gowda, B.H.J.; Kumar, S.; Raikar, A.S.; Masand, P.; Garg, A.; Goswami, P.; Kahwa, I. Overview of processed excipients in ocular drug delivery: Opportunities so far and bottlenecks. *Heliyon* **2024**, *10*, e23810, https://doi.org/10.1016/j.heliyon.2023.e23810.
21. Sumathi, S.; Ray, A.R. Release behaviour of drugs from tamarind seed polysaccharide tablets. *J. Pharm. Pharm. Sci.* **2002**, *5*, 12–18.
22. Blynskaya, E.V.; Tishkov, S.V.; Vinogradov, V.P.; Alekseev, K.V.; Marakhova, A.I.; Vetcher, A.A. Polymeric Excipients in the Technology of Floating Drug Delivery Systems. *Pharmaceutics* **2022**, *14*, 2779, https://doi.org/10.3390/pharmaceutics14122779.
23. Srivastava, A.K.; Wadhwa, S.; Ridhurkar, D.; Mishra, B. Oral Sustained Delivery of Atenolol from Floating Matrix Tablets—Formulation and In Vitro Evaluation. *Drug Dev. Ind. Pharm.* **2005**, *31*, 367-374, https://doi.org/10.1081/DDC-54313.
24. Bongiovanni Abel, S.; Busatto, C.A.; Karp, F.; Estenoz, D.; Calderón, M. Weaving the next generation of (bio)materials: Semi-interpenetrated and interpenetrated polymeric networks for biomedical applications. *Adv. Colloid Interface Sci.* **2023**, *321*, 103026, https://doi.org/10.1016/j.cis.2023.103026.
25. Rokhade, A.P.; Agnihotri, S.A.; Patil, S.A.; Mallikarjuna, N.N.; Kulkarni, P.V.; Aminabhavi, T.M. Semi-interpenetrating polymer network microspheres of gelatin and sodium carboxymethyl cellulose for controlled release of ketorolac tromethamine. *Carbohydr. Polym.* **2006**, *65*, 243-252, https://doi.org/10.1016/j.carbpol.2006.01.013.
26. Kozlowska, J.; Prus-Walendziak, W.; Stachowiak, N.; Bajek, A.; Kazmierski, L.; Tylkowski, B. Modification of Collagen/Gelatin/Hydroxyethyl Cellulose-Based Materials by Addition of Herbal Extract-Loaded Microspheres Made from Gellan Gum and Xanthan Gum. *Materials* **2020**, *13*, 3507, https://doi.org/10.3390/ma13163507.
27. Taboun, A.; Jovanovic, M.; Petrovic, M.; Stajcic, I.; Pesic, I.; Stojanovic, D.B.; Radojevic, V. Citric Acid Cross-Linked Gelatin-Based Composites with Improved Microhardness. *Polymers* **2024**, *16*, 1077, https://doi.org/10.3390/polym16081077.
28. Reddy, O.S.; Subha, M.; Jithendra, T.; Madhavi, C.; Rao, K.C. Fabrication and characterization of smart karaya gum/sodium alginate semi-IPN microbeads for controlled release of D-penicillamine drug. *Polym. Polym. Compos.* **2020**, *29*, 163-175, https://doi.org/10.1177/0967391120904477.
29. Hadke, J.; Shagufta, K. Preparation of *Sterculia foetida*-pullulan-Based Semi-interpenetrating Polymer Network Gastroretentive Microspheres of Amoxicillin Trihydrate and Optimization by Response Surface Methodology. *Turk. J. Pharm. Sci.* **2021**, *18*, 388, https://doi.org/10.4274/tjps.galenos.2020.33341.
30. Rampado, R.; Peer, D. Design of Experiments in the Optimization of Nanoparticle-Based Drug Delivery Systems. *J. Control. Release* **2023**, *358*, 398–419, doi.org

31. Rokhade, A.P.; Shelke, N.B.; Patil, S.A.; Aminabhavi, T.M. Novel interpenetrating polymer network microspheres of chitosan and methylcellulose for controlled release of theophylline. *Carbohydr. Polym.* **2007**, *69*, 678-687, https://doi.org/10.1016/j.carbpol.2007.02.008.
32. Dwiastuti, R.; Suhendra, P.A.; Yuliani, S.H.; Riswanto, F.D.O. Application of the central composite design approach for optimization of the nanosilver formula using a natural bioreductor from Camellia sinensis L. extract. *J. Appl. Pharm. Sci.* **2022**, *12*, 048-056, https://doi.org/10.7324/JAPS.2022.120806.
33. Somadasan, S.; Subramaniyan, G.; Athisayaraj, M.S.; Sukumaran, S.K. Central Composite Design: An Optimization Tool for Developing Pharmaceutical Formulations. *J. Young Pharm.* **2024**, *16*, 400-409, https://doi.org/10.5530/jyp.2024.16.52.
34. Wadher, K.J.; Kakde, R.B.; Umekar, M.J. Formulation and Evaluation of a Sustained-Release Tablets of Metformin Hydrochloride Using Hydrophilic Synthetic and Hydrophobic Natural Polymers. *Indian J. Pharm. Sci.* 2011, *73*(2), 208–215, https://doi.org/10.4103/0250-474x.91579
35. Verma, R.; Gupta, A.K.; Sharma, V.; Gupta, M.K. A Review: Formulation and Optimization of Sustained Release Eudragit Coated Metformin Hydrochloride. J. Drug Deliv. Ther. 2019, 9, 663-666, http://dx.doi.org/10.22270/jddt.v9i4.3074.
36. Wang, J.; Tan, J.; Chen, L.; Zhang, S.; Gao, H. Oral delivery of metformin by chitosan nanoparticles for polycystic kidney disease. J. Control. Release. 2021, 329, 1198-1209, doi:10.1016/j.jconrel.2020.10.047.
37. Patil, M.; Sonawane, D.; Sonawane, S.; Bhambere, D.; Kshirsagar, S. Application of Central Composite Design for Development of Celecoxib Loaded Lipospheres: Formulation and in-vitro Characterization. Indian J. Pharm. Educ. Res. 2022, 56, 405-413.
38. Kaur, M.; Sharma, A.; Puri, V.; Aggarwal, G.; Maman, P.; Huanbutta, K.; Nagpal, M.; Sangnim, T. Chitosan-Based Polymer Blends for Drug Delivery Systems. *Polymers* **2023**, *15*, 2028, https://doi.org/10.3390/polym15092028.
39. Lavelle, E.C. Targeted delivery of drugs to the gastrointestinal tract. *Crit. Rev. Ther. Drug Carrier Syst.* **2001**, *18*, https://doi.org/10.1615/CritRevTherDrugCarrierSyst.v18.i4.10.
40. Fares, M.M.; Assaf, S.M.; Abul-Haija, Y.M. Pectin grafted poly(*N*-vinylpyrrolidone): Optimization and *in vitro* controllable theophylline drug release. *J. Appl. Polym. Sci.* **2010**, *117*, 1945-1954, https://doi.org/10.1002/app.32172.
41. Patil, J.S.; Gujar, K.N.; Patil, S.B. Ionotropically Gelled Chitosan-alginate Complex Hydrogel Beads: Preparation, Characterization and In Vitro Evaluation. *Int. J. Pharm. Ed. Res.* **2011**, *46*, 321-329.
42. Abdel-Kader, H.; Al-Kassas, R.S.; Al-Gohary, O.M. Effect of Eudragit RS on the Release Behaviour of Theophylline from Matrix Tablets Prepared by Solvent Evaporation Technique. *Saudi Pharm. J.* **2017**, *25*, 87-95.
43. Draganoiu, E; Muça, B; Stansbrey,A.; Luo,H.; Wilber,W.; Guo, H. Effect of Carbomer and hydroxypropyl methylcellulose combination on drug release from matrix tablets. *Eur. J. Pharm. Sci*. **2005**, *25*, S222-S223.

Publisher's Note & Disclaimer